

## Collection 5 Changes to MODIS Cloud Mask (35\_L2)

Significant improvements have been made to the MODIS cloud mask (MOD35) in preparation for Collection 5 reprocessing and forward stream data production. Most of the modifications are realized for nighttime scenes where polar and oceanic regions will see marked improvement. For polar night scenes, two new spectral tests using the 7.2  $\mu\text{m}$  water vapor absorption band have been added as well as updates to the 3.9-12  $\mu\text{m}$  and 11-12  $\mu\text{m}$  cloud tests. More non-MODIS ancillary data has been added for nighttime processing. Land and sea surface temperature maps provide crucial information for middle and low-level cloud detection and lessen dependence on ocean brightness temperature variability tests. Sun-glint areas are also improved by use of sea surface temperatures to aid in resolving observations with conflicting cloud vs. clear-sky signals, where visible and NIR reflectances are high, but infrared brightness temperatures are relatively warm. Day vs. night sea surface temperatures derived from MODIS radiances and using only the MODIS cloud mask for cloud screening are contrasted. Frequencies of cloud from sun-glint regions are shown as a function of sun-glint angle to gain a sense of cloud mask quality in those regions.

### CLOUD MASK ENHANCEMENTS

#### Polar Night

Discriminating clear sky from cloudy conditions is nowhere more difficult than under conditions of polar night. Besides very small or non-existent thermal contrast between clouds and surface and persistent temperature inversions, the extremely cold temperatures make accurate instrument calibration challenging. Two spectral cloud tests were modified, one was added, and one clear-sky restoral test was added.

#### 11–3.9 $\mu\text{m}$ Brightness Temperature Difference (BTD) Low Cloud Test

The 11–3.9  $\mu\text{m}$  BTD low cloud test is based on the differential absorption between these two wavelengths by both water and ice cloud particles. The (nighttime) BTD may be either negative or positive depending on cloud optical depth and particle size<sup>1</sup>. The situation becomes more complex in temperature inversions, however, which are frequent in polar night conditions. For a complete discussion of the problem, see Liu<sup>1</sup>. Previous 11-3.9  $\mu\text{m}$  test thresholds did not take temperature inversions into account and were most appropriate for non-polar, thick water clouds. For Collection 5 polar night, the confident cloud thresholds vary linearly from  $-0.8$  to  $+0.6$  as the 11  $\mu\text{m}$  brightness temperature (BT) varies between 235K and 265K. The threshold is constant below 235K and above 265K. This assumes that more inversions are found as surface temperatures decrease. Figure 1b shows an example of test results on April 1, 2003 beginning at 05:05 UTC from northwest Canada. Figure 1a shows imagery of MODIS 11  $\mu\text{m}$  BTs for the same scene. Note that north is at the bottom and west is to the right in these images. In all test result figures, white means cloud indicated, gray means no cloud indicated and black means test not performed.

#### 3.9-12 $\mu\text{m}$ BTD High Cloud Test

The 3.9-12  $\mu\text{m}$  BTD high cloud test has been modified for polar night conditions. For reasons not well understood, the thresholds for this test need to increase with decreasing temperatures below 265K. This is counter-intuitive from arguments based on atmospheric water vapor loading and absorption at these two wavelengths. Perhaps the calibration of one or both bands is of reduced accuracy at cold temperatures. In addition, the test cannot be used on the very coldest and driest scenes such as are found in Antarctica and Greenland during the winter season. Therefore, the test is not performed in polar night conditions when the elevation exceeds 2000 m. The Collection 5 confident cloud threshold varies linearly from  $+4.5\text{K}$  to  $+2.5\text{K}$  as the 11  $\mu\text{m}$  BT varies between 235K and 265K. The threshold is constant below 235K and above 265K. Figure 1d shows an example of test results from the same scene as above.

#### 11-12 $\mu\text{m}$ BTD Thin Cirrus Test

Previous versions of the cloud mask algorithm made use of this test only over surfaces not covered by snow or ice. The Collection 5 test makes use of thresholds taken from Key<sup>2</sup> who extended the Saunders and Kriebel<sup>3</sup> values to very low temperatures. The modified test has replaced the original in all processing paths for both day and night processing except for Antarctica. Figure 1c shows example results from the same scene as above. At these very cold scene temperatures, the 11-12  $\mu\text{m}$  BT starts to become noisy as seen at middle left.

### 7.2-11 $\mu\text{m}$ BT Cloud Test

The most significant change to the polar night algorithm is the addition of a new 7.2-11 $\mu\text{m}$  BT cloud test. Since the weighting function of the 7.2  $\mu\text{m}$  band peaks at about 800 hPa, the BT is related to the temperature difference between the 800 hPa layer and the surface, which the 11  $\mu\text{m}$  band is most sensitive to. In the presence of low clouds under polar night conditions with a temperature inversion, radiation from the 11  $\mu\text{m}$  band comes primarily from the relatively warm cloud top, decreasing the 7.2-11  $\mu\text{m}$  BT compared to the clear-sky value. For a complete discussion of the theory, see Liu<sup>1</sup>. In conditions of deep polar night, even high clouds may be warmer than the surface and will often be detected with this test. The test as configured in MOD35 is applicable only over nighttime snow and ice surfaces. Because the 7.2  $\mu\text{m}$  band is sensitive to atmospheric water vapor and also because inversion strength tends to increase with decreasing surface temperatures<sup>1</sup>, thresholds for this test are a function of the observed 11  $\mu\text{m}$  BT. The thresholds vary linearly in three ranges: BT +2K to -4.5K for 11  $\mu\text{m}$  between 220K and 245K, BT -4.5K to -11.5K for 11  $\mu\text{m}$  between 245 and 255K, and BT -11.5 to -21K for 11  $\mu\text{m}$  between 255K and 265K. Thresholds are constant for 11  $\mu\text{m}$  below 220K or above 265K. The thresholds are slightly different over ice (frozen water surfaces): BT +2K to -4.5K for 11  $\mu\text{m}$  between 220K and 245K, BT -4.5K to -17.5K for 11  $\mu\text{m}$  between 245 and 255K, and BT -17.5 to -21K for 11  $\mu\text{m}$  between 255K and 265K. These somewhat larger BTs presumably reflect a lesser tendency for strong inversions and higher water vapor loading over frozen water surfaces as opposed to snow-covered land areas. These thresholds also differ slightly from those reported in Liu<sup>1</sup>, a result of extensive testing over many scenes and the necessity of meshing this test with other cloud mask tests and algorithms. Note that this test was also implemented for non-polar (latitude < 60 deg.), nighttime snow-covered land. Figure 1e shows imagery from the 7.2  $\mu\text{m}$  band for this same scene from Canada and 1f shows the results of the test. Note the difference in texture between cloudy and clear on the right in the 7.2  $\mu\text{m}$  BT imagery, even though the gray scale indicates similar temperatures for much of the scene. Clouds indicated on the left are just barely seen in Figure 1a.

### 7.2-11 $\mu\text{m}$ BT Clear Sky Test

A 7.2-11  $\mu\text{m}$  BT test may also be utilized to find clear sky because of the prevalence of polar night temperature inversions. This test works in the same way as the current 6.7-11  $\mu\text{m}$  BT clear-sky restoral test, where 11  $\mu\text{m}$  BTs are sometimes significantly lower than those measured in the 6.7  $\mu\text{m}$  band because the 6.7  $\mu\text{m}$  weighting function peaks near the top of a warmer inversion layer in some cases. However, since the 7.2  $\mu\text{m}$  band peaks lower in the atmosphere, a 7.2-11  $\mu\text{m}$  BT test can detect lower and weaker inversions. Pixels are restored to clear if the 7.2-11  $\mu\text{m}$  BT > 5K.

Verifying cloud detection results under polar night conditions is very difficult without human observations or active sensors to compare with. Both are almost totally absent in polar winter. Figure 4 shows both the underlying problem in cloud detection for polar night and an indication of cloud mask results. It shows a histogram of observed BTs from one MODIS granule (open bars) over frozen ocean near the North Pole. Also shown are the amounts of confident clear and confident cloudy retrievals for each BT class. Instead of clear-sky observations making a distinct peak on the warm end of the histogram as in most Earth scenes, this shows a more Gaussian distribution with most values (both clear and cloudy) somewhere in the middle. However, as shown in the figure, in a given region one expects temperatures and water vapor loading in clear skies over the surface ice to be relatively uniform so that a majority of those BTs will fall in one 5K-wide class. This was verified by inspection of the imagery for this granule. Note that many, if not most of the confident cloudy BTs were in either the same or warmer BT classes as that of the clear-sky peak, indicating the lack of thermal contrast that is the fundamental cloud detection problem for polar night. Liu<sup>1</sup> compared ground-based radar/lidar data to MODIS cloud mask results using the new polar night spectral tests and those from Collection 4 and

found that the misidentification rate of cloud as clear decreased from 44.2% to 16.3% in the Arctic. The misidentification of clear as cloud remained at about 8%.

### **Nighttime Land**

The major enhancement to nighttime land processing is the inclusion of a surface temperature (SFCT) test. Gridded surface air temperatures from Global Data Assimilation System<sup>4</sup> (GDAS) model output fields are compared to observed 11  $\mu\text{m}$  BTs. Due to large variations of SFCT in mountainous areas and large diurnal swings in desert regions that are not always well characterized in the gridded data, the test is not performed there. Even with these restrictions, great care must be taken when applying this test. Thresholds of GDAS SFCT-11  $\mu\text{m}$  BT are set at 12K for vegetated areas and 20K for semi-arid lands but are adjusted for viewing zenith angle and water vapor loading based on 11-12  $\mu\text{m}$  BTs. With threshold values set this high, the test can obviously function only as a gross cloud test. But it is particularly useful for detecting thick mid-level clouds that are surprisingly difficult to detect at night over land. The test is also performed on snow-free polar scenes.

### **Nighttime Ocean**

Nighttime ocean cloud detection has undergone major changes. A sea-surface temperature (SST) test and an 8.6-7.2  $\mu\text{m}$  BT test have been implemented for the first time. A new 11  $\mu\text{m}$  BT variability test has also been included. The ocean Reynolds<sup>5</sup> SST-11  $\mu\text{m}$  BT test has the same function as the land surface temperature test, namely as a gross cloud test. Because of the more uniform ocean surface temperatures the threshold can be lowered to a base value of 6K that is adjusted to account for viewing zenith angle and water vapor loading.

An 8.6-7.2  $\mu\text{m}$  BT test has been added and is designed primarily to detect thick mid-level clouds but can also detect lower clouds in regions of low relative humidity in the middle atmosphere. It is sometimes more effective than the SST test for finding stratocumulus clouds of small horizontal extent. It can also detect high, thick clouds. Both this and the SST test are needed in order to find those clouds that are thick but that also show very small thermal spatial variability. The test thresholds are 16.0K, 17.0K, and 18.0K for 0.0, 0.5, and 1.0 confidence of clear sky, respectively.

The 11  $\mu\text{m}$  variability test has been modified to detect clouds of small spatial extent (a pixel or two) and cloud edges. Most thick clouds are now found by other tests but a variability test is very effective at night for detecting the thinner, warmer cloud edges over the uniform ocean surface. The previous (Collection 4) test determined a standard deviation over the pixel of interest and the eight surrounding. Then, a very stringent threshold was used to determine cloudiness. In the Collection 5 version, the number of differences  $\leq 0.5\text{K}$  in 11  $\mu\text{m}$  BT between each surrounding pixel and the center one are counted. The higher the number (8 possible), the more likely the center pixel is clear. The confident cloud and confident clear thresholds are 3 and 7, respectively. Figure 2a-2d shows examples of an ocean scene with widespread stratus clouds in the subtropical southern Pacific west of South America and results of the three tests discussed.

The quality of the MODIS nighttime ocean cloud mask algorithm has seen a major improvement. The changes noted above have lowered the retrieved cloud amounts to reasonable levels and compare favorably with daytime values. This is a result of better detection of above-freezing clouds and use of less stringent BT variability thresholds. Figure 6a shows zonal mean values of nighttime ocean clear-sky frequencies for one day from Terra Collection 4 and 5 algorithms. Though the locations of minima and maxima stay the same, clear sky amounts increase by as much as 10% over the southern ocean and by as much as 20% over the northern subtropics.

To further investigate the quality and consistency of the nighttime ocean cloud mask, sea surface temperatures (SSTs) were computed and analyzed for the eastern Pacific (-45 to +45 latitude and 180 to 130 west longitude) over an eight-day period from April 1-8, 2003. Single-pixel values from day and night were calculated separately, then binned into 0.25K latitude and longitude regions and compared with each other, as well as to the Reynolds SST data from the same locations and times. The current MODIS SST equation and coefficients<sup>6</sup> were used (but not the entire algorithm) along with clear-sky 11  $\mu\text{m}$  BTs and 11-12  $\mu\text{m}$  BTs, where clear-sky was determined solely from the C5 MODIS cloud

mask (probably clear and confident clear designations). No 4  $\mu\text{m}$  data was used at night and no pre-processing or post-processing screening was performed except to eliminate obviously bad radiance data. The purpose of this exercise was not to produce the best SST possible, but rather to show that the ocean cloud mask performs well and is reasonably consistent between day and night. Figure 6b shows a histogram of SST values obtained for day and night in 0.25K classes. The difference in the peak class between day and night is 0.25K. Figure 6c shows a histogram with the same class widths but where the MODIS SSTs were compared to those of the Reynolds data set. The Reynolds values did not change from day to night. The peak in the difference (MODIS – Reynolds) distribution lies at  $-0.25\text{K}$  for both day and night, though there are less nighttime values for all difference classes warmer than the peak value and more for all less than the peak. This is undoubtedly mostly due to a little more cloud contamination in the nighttime clear-sky BTs, though direct observations of SST show a diurnal cycle of up to a degree or so in some situations<sup>7</sup>. Nevertheless, 82.1% of daytime and 68.6% of nighttime MODIS SSTs are within 1 degree of the Reynolds-Blended values on average, using nothing but MOD35 to determine the input BTs. Figure 6d shows the zonal mean daytime MODIS SSTs and day minus night differences. The fit to the differences is a 5<sup>th</sup>-order polynomial. Note that though the largest day vs. night differences in Figure 6b is greatest in the warmest regions, the mean latitudinal difference there is only 0.25K. The larger zonal mean differences are seen in higher latitudes to both north and south where more clouds are present and SSTs are lower. This is an indication that cloud edges are not as effectively screened out by the nighttime algorithm. From Figure 5b one can see that, for the MOD35 algorithm, about 10% of ocean cloudy pixels are detectable only by use of visible and NIR data.

### Sun-glint and Daytime Ocean

Improvements have been made to the cloud mask in sun-glint regions and in daytime oceans generally. The SST test has been implemented in the daytime ocean algorithm exactly as in the nighttime case. For areas not affected by sun-glint, the improvements are small since the algorithm has already been well developed for some time. The most noticeable change is more confident cloud and less uncertain for scenes containing thin cirrus. The changes are more dramatic for sun-glint regions, however. Many low-level clouds with above-freezing cloud top temperatures have been moved from the uncertain to the confident cloud category by use of the SST test. Much of the ambiguity between bright clouds and sometimes equally bright ocean surfaces on the one hand, and between warm clouds and warm ocean surfaces on the other, is ameliorated by knowledge of the SST.

In addition, a new clear-sky restoral test is applied. When no thermal tests indicate the presence of cloud, the mean and standard deviation of 0.86  $\mu\text{m}$  reflectances are computed over the pixel of interest and the eight surrounding. Pixels are declared probably clear (confidence 0.96) when the standard deviation multiplied by the mean is  $< 0.001$ . This has the effect of restoring to clear many pixels which are bright in the visible and NIR and also thermally very uniform. This test is performed in addition to previously existing restoral tests. Figure 3 shows an example where the new algorithm greatly improves the cloud mask results.

To demonstrate the improvements in the cloud mask sun-glint algorithm and the consistency of results between sun-glint and non sun-glint pixels, a region of the Pacific Ocean between  $-30$  and  $+45$  latitude was chosen for a detailed study. The longitudinal domain was  $-180$  to  $-130$  (minus = west) and the temporal range was April 1-8, 2003. Figure 5a shows total cloud amount as a function of glint angle (binned in 6-degree increments). Sun-glint is defined in the cloud mask process as glint angles from 0 to 36 degrees, where 0 defines the specular point. Because increasing sun-glint angles on the Earth's surface are characterized by a series of concentric circles, larger glint angles also imply a wider range of latitudes, as well as increasing surface area and viewing zenith angles. At first glance, the total cloud amount from the combined confident cloudy and uncertain decisions from MOD35 (top curve) would appear to be seriously biased in the sun-glint regions, but other indications of cloud (bottom curves) show the same pattern. Sub-freezing observations in the 11  $\mu\text{m}$  band are independent of sun-glint, and thin and thick cirrus as determined by 1.38  $\mu\text{m}$  reflectances, are generally very insensitive to glint especially in moist, tropical regions. The numbers in brackets along the top curve indicate the minimum and maximum latitudes from which the corresponding values originated. Figure 5b shows total cloud frequency from the same region but from non-glnt pixels and as a function of latitude. It can be seen from comparing the latitude ranges from the first plot to the cloud frequencies of those latitudes on the second, that the trend toward lower cloud amounts in the latitudes most affected by glint is reasonable. Using the total number of observations from each glint angle bin as a surrogate for areal coverage (not exact), a reasonably accurate

weighted average may be obtained over the entire region. The non-glint cloud amount was 70.8% while the cloud percentage from the glint region was 64.5%, a difference of 6.3%. Although not proven by this analysis, we suspect that the majority of missed cloudy pixels in glint areas are those warm clouds of small extent that are detected only by visible and NIR cloud tests. In areas affected by glint, the background ocean reflectance is often greater than that from these clouds, rendering them invisible. The bottom curve on Figure 5b shows zonal means of the frequencies of these clouds as defined by the cloud mask from non-glint regions.

### **Polar Daytime Snow**

A new version of the 3.9-11  $\mu\text{m}$  test has been developed for polar, daytime conditions. The test thresholds are now dependent on the observed 11  $\mu\text{m}$  BT when that BT is lower than 245K. Also, the test will no longer be performed at all when the 11  $\mu\text{m}$  BT is below 230K. During Arctic and Antarctic spring and autumn seasons, the sun is above the horizon but surface temperatures and hence clear-sky observed BTs are still very low, sometimes < 200K at 11  $\mu\text{m}$  on the Antarctic plateau near the South Pole. Under these conditions, and adding just a small amount of solar insolation, the extreme nonlinearity of the Planck function at 3.9  $\mu\text{m}$  makes the 3.9-11  $\mu\text{m}$  BTD higher than one would expect for clear-sky observations at warmer temperatures. This effect, along with the use of static test thresholds was leading to false cloud determinations in Antarctica and Greenland. The new thresholds will vary between 7.0K and 14.5K as 11  $\mu\text{m}$  BTs vary between 245K and 230K at the 0.5 clear-sky confidence level. Above 245K, the threshold will remain as before, at 7K.

### **Clear-sky Radiance Statistics and Bias**

Beginning with Collection 5 processing, a new program will generate clear-sky radiances from cloud mask results (PGE55). Previously, they were output from MOD35 directly, but a decision to output more bands and to generate biases with respect to forward model radiance calculations necessitated the change. Daily and 8-day composites will be computed for bands 1-7 and 17-36 at 25-km resolution. Statistics for each 25-km equal-area bin will include:

- Total number of observations
- Number of clear observations
- Sum of clear values
- Minimum clear value
- Maximum clear value
- Sum of viewing zenith angles
- Sum of clear-sky values squared
- Sum of observed clear minus calculated clear values (for clear-sky bias calculations)
- Sum of observed minus calculated clear values squared

As before, a primary use of the clear-sky products will be quality control of the cloud mask. In addition, clear-sky reflectances/radiances could be used in shadow determination and temporal consistency checks, when averaged into daily or eight-day gridded products. Biases between calculated and observed radiances in the 15  $\mu\text{m}$  CO<sub>2</sub> absorption band will be collected over eight-day periods and used as input to the cloud top properties algorithm (MOD06), specifically for cloud top pressure determinations.

## **REFERENCES**

1. Y. Liu, J. Key, R. Frey, S. Ackerman, and W. Menzel, "Nighttime polar cloud detection with MODIS", Remote sensing of environment, **92**, 181-194, 2004.
2. J. Key, "The cloud and surface parameter retrieval (CASPR) system for polar AVHRR", University of Wisconsin, Madison, WI, 2002.

3. R. Saunders and K. Kriebel, "An improved method for detecting clear sky and cloudy radiances from AVHRR data", *International Journal of Remote Sensing*, **9**, 123-150, 1988.
4. J. Derber, D. Parrish, and S. Lord, "The new global operational analysis system at the National Meteorological Center", *Weather and Forecasting*, **6**, 538-547.
5. R. Reynolds, and T. Smith, "Improved global sea surface temperature analyses", *Journal of Climate*, **7**, 929-948, 1994.
6. O. Brown, P. Minnett, R. Evans, E. Kearns, K. Kilpatrick, A. Kumar, R. Sikorski, and A. Závody, "Algorithm theoretical basis document", EOS ATBD web site, 1999.
7. P. Webster, C. Clayson, and J. Curry, "Clouds, radiation, and the diurnal cycle of sea surface temperature in the tropical western Pacific", *Proceedings of the Fifth Atmospheric Radiation Measurement (ARM) Science Team Meeting*, *DOE CONF-9503140*, ARM Science Team Meeting Proceedings web site, 1995.

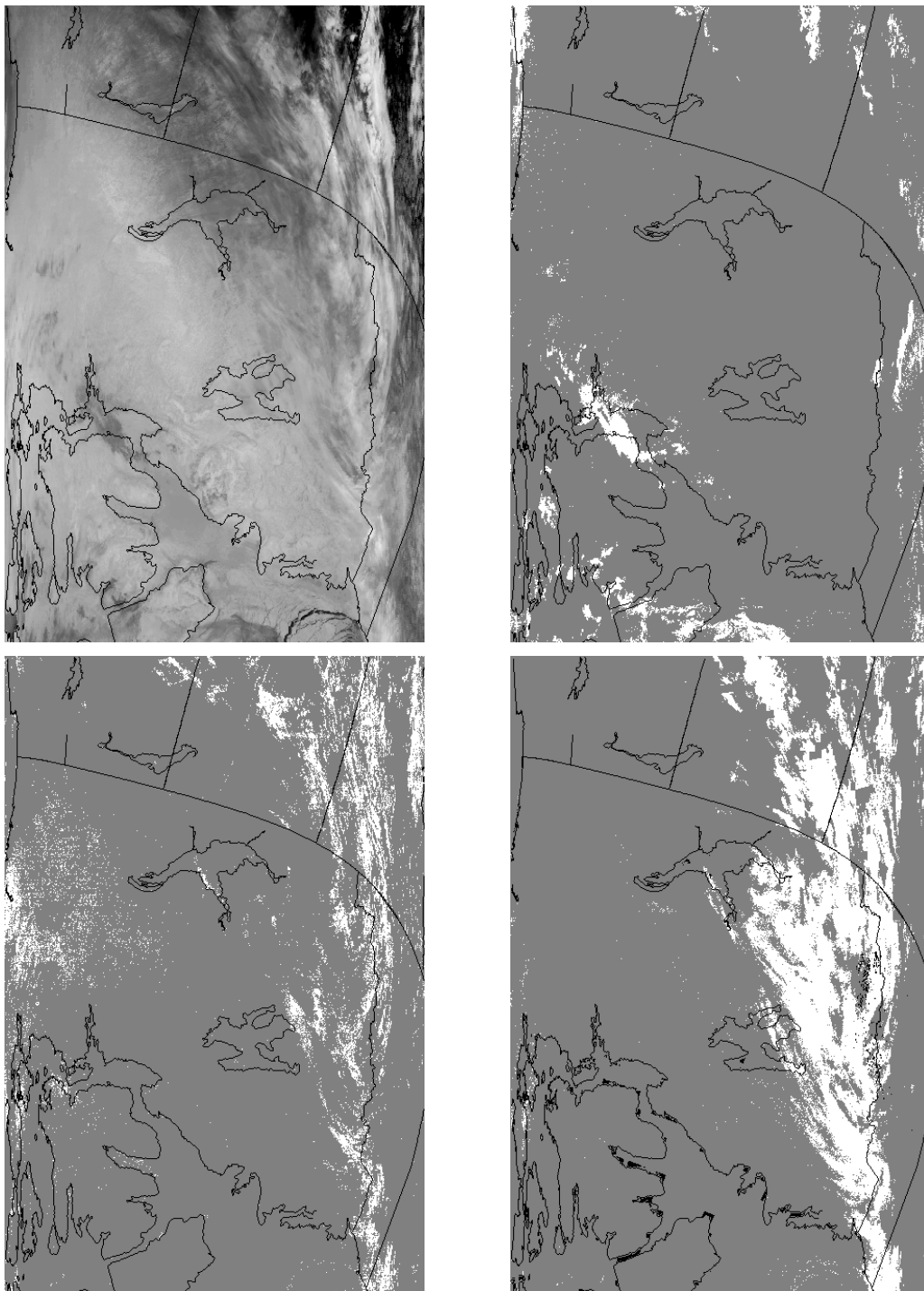


Figure 1 a-d: Left to right, top and bottom: MODIS 11  $\mu\text{m}$  BT image (a), 11-3.9  $\mu\text{m}$  BTD test (b), 11-12  $\mu\text{m}$  BTD test (c), and 3.9-12  $\mu\text{m}$  BTD test (d). Scene is from 05:05 UTC, April 1, 2003.

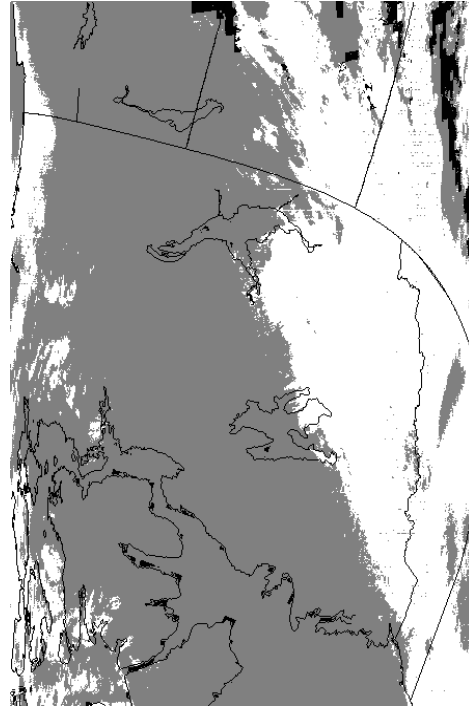
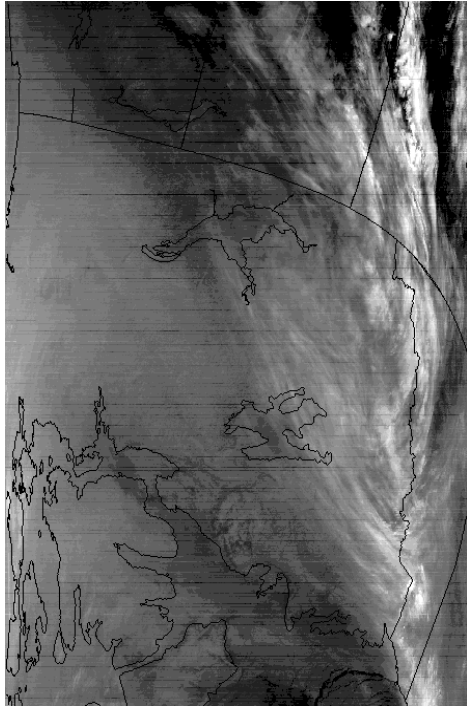


Figure 1 e and f: MODIS 7.2  $\mu\text{m}$  BT image (e) and 7.2-11  $\mu\text{m}$  BTD test (f).

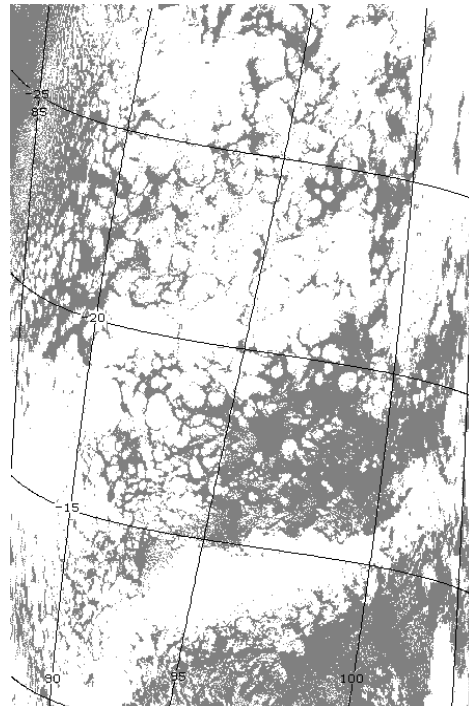
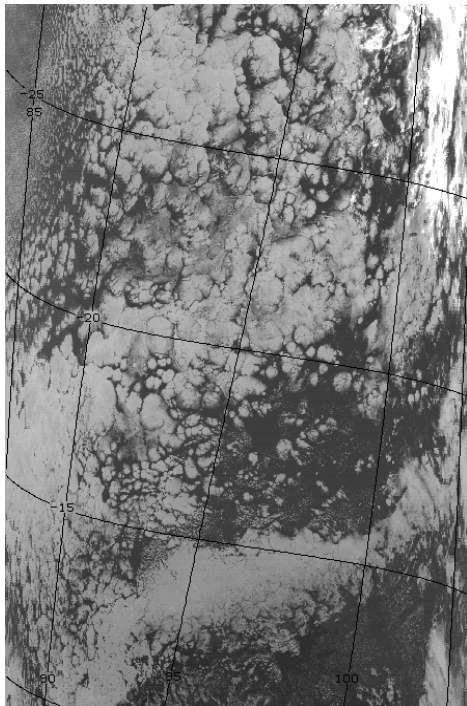


Figure 2 a and b: MODIS 3.9  $\mu\text{m}$  BT image (a), and SST test (b). Scene is from 05:00 UTC, April 6, 2003.

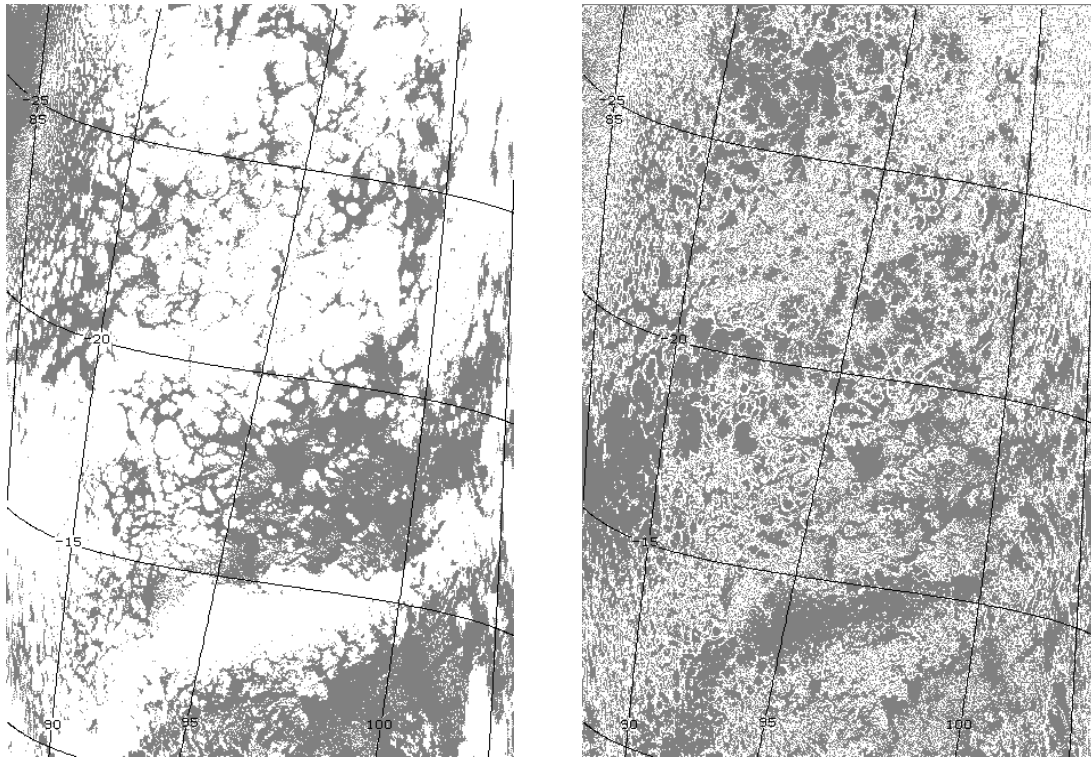


Figure 2 c and d: MODIS 8.6-7.2  $\mu\text{m}$  BTD test (c), and 11  $\mu\text{m}$  variability test (d) for scene shown in 2a.

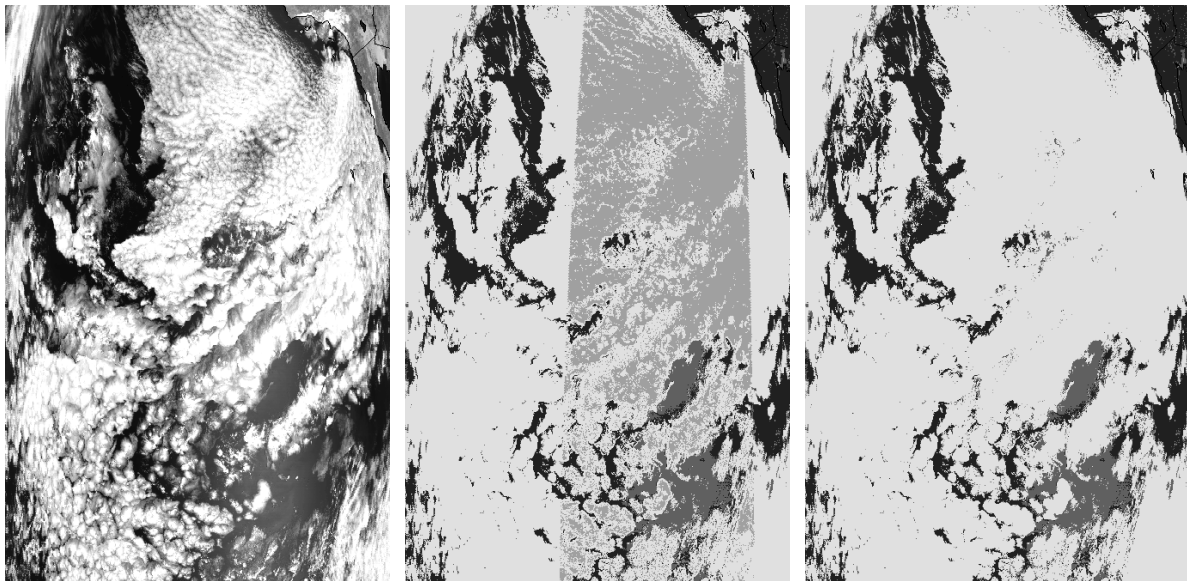


Figure 3 a-c: MODIS 0.86  $\mu\text{m}$  image (a), Collection 4 cloud mask (b), and Collection 5 mask result (c). In the mask images, black is confident clear, dark gray is probably clear, light gray is uncertain, and white is confident cloud. Baja California may be seen in (a) in the upper right corner of the image. Scene is from April 6, 2004 at 19:10 UTC.

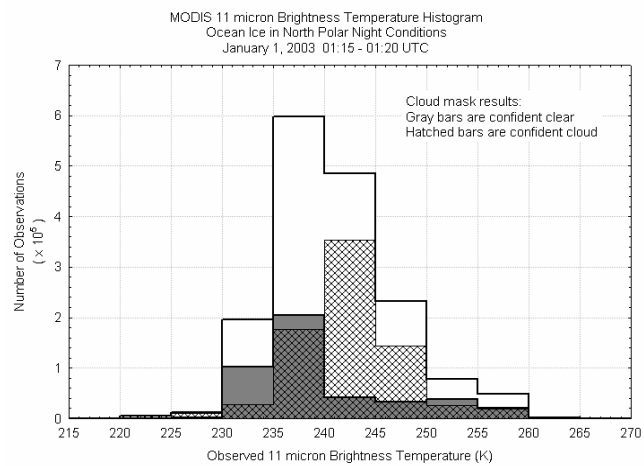


Figure 4: Histogram of 11  $\mu\text{m}$  BTs over frozen ocean from January 1, 2003 near the North Pole.

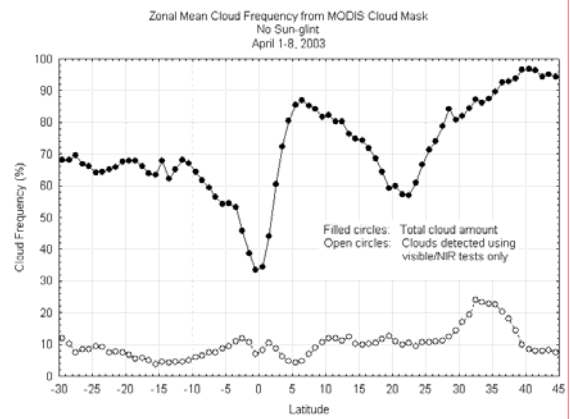
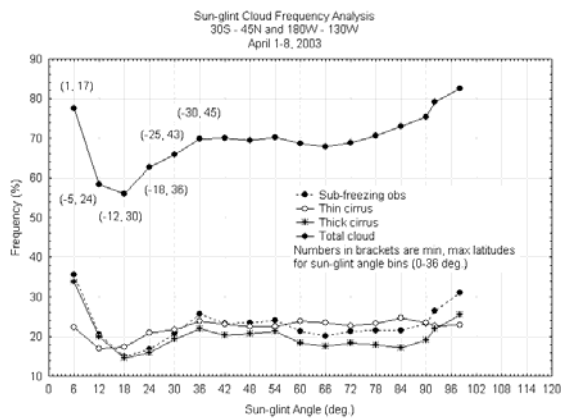


Figure 5 a and b: Cloud frequencies as a function of sun-glint angle (a) and as a function of latitude (b). The cloud frequencies in (b) do not contain any observations from sun-glint conditions. Data is from April 1-8, 2003.

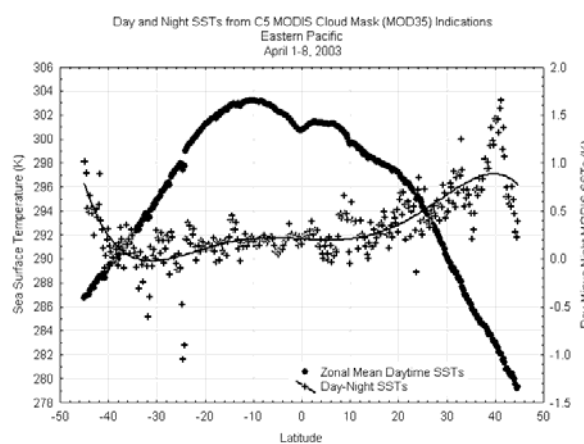
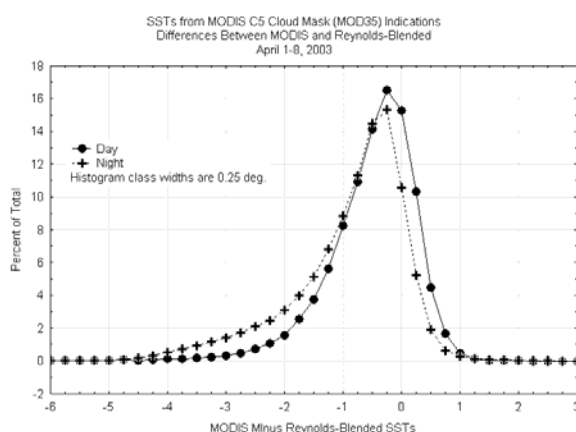
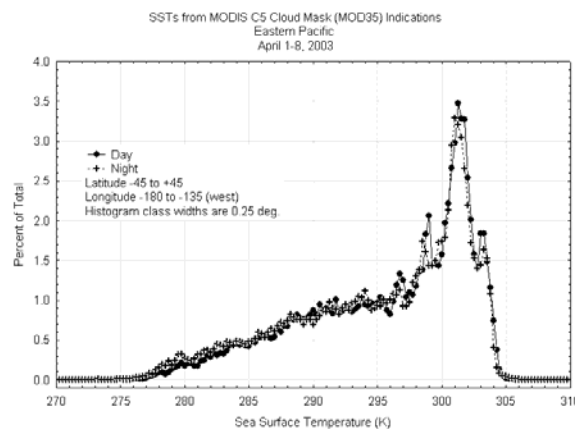
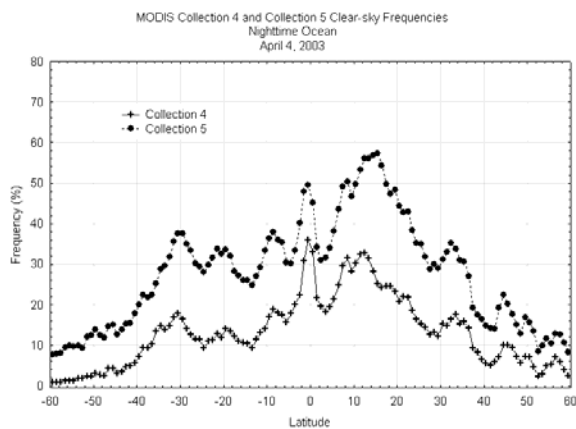


Figure 6 a-d: Left to right, top and bottom: zonal mean nighttime ocean clear-sky frequency from MODIS Collections 4 and 5 for April 4, 2003 (a), histogram of day and night SSTs using the same SST algorithm and coefficients (b), histogram of MODIS vs. Reynolds-Blended SSTs for day and night (c), and zonal mean daytime SSTs and zonal mean day minus night SSTs (d). SST analysis uses data from the eastern Pacific Ocean (-45 to +45 latitude and -180 to -130 longitude) from April 1-8, 2003. Clear skies determined solely from Collection 5 MODIS cloud mask (MOD35).